The 8th European Congress on Computational Methods in Applied Sciences and Engineering
ECCOMAS Congress 2022
5–-9 June 2022, Oslo, Norway

SIMULATION OF WIND INDUCED EXCITATION OF A MEMBRANE STRUCTURE WITH PONDING WATER

NAVANEETH K. NARAYANAN[1], ROLAND WÜCHNER[2] AND JORIS DEGROOTE[1,3]

[1]Department of Electromechanical, Systems and Metal Engineering, Ghent University
Sint-Pietersnieuwstraat 41, 9000 Ghent, Belgium
e-mail: navaneeth.narayanan@ugent.be

[2] Institut für Statik und Dynamik, Technische Universität Braunschweig
Beethovenstraße 51, 38106 Braunschweig, Germany

[3] Flanders Make, Belgium

Key words: Partitioned FSI, Volume Of Fluid, Ponding, Membrane structure, Wind gust

Abstract. This paper proposes a new partitioned coupling approach to simulate the wind induced excitation of a membrane structure with ponding water. This approach uses three different solvers to simulate wind, water and membrane structure. The main assumption here is that the interaction between the wind and water can be neglected due to the small depth and small fetch of the water, relative to the size of the membrane structure. This assumption results in a coupling strategy where the structural solver independently interacts with the wind and water solver. The results from this method is compared with a straightforward approach, where a two-phase solver, modeling the wind and water, is coupled to a structural solver. The obtained results agreed very well with the reference modeling approach, where all the interactions are taken into account. Furthermore, the proposed method was found to be computationally more efficient.

1 INTRODUCTION

Membrane structures undergo large deformation to carry loads and consequently they can be vulnerable to ponding. When coupled with a strong wind gust, this can lead to violent excitation of the tent structure. One example of this phenomenon was observed during the 2011 Pukkelpop festival held in Kiewit, where the sudden onset of a storm along with heavy rainfall [1] damaged many tents and also resulted in casualties. This is clearly a fluid-structure interaction (FSI) phenomenon involving coupling of a membrane structure, ponding water and the wind. Based on a literature survey, the authors found several publications on numerical studies of the interaction of wind and a flexible structure [2, 3, 4, 5]. There are also considerable numerical studies performed on the interaction of a flexible structure and a dense fluid with a free surface [6, 7, 8, 9, 10, 11]. However, to the best of the authors' knowledge, simulations involving wind, water, and a flexible structure are non-existent in the literature. Therefore, this paper attempts to fill this knowledge gap.

In our previous work [12], we developed partitioned and monolithic algorithms to calculate the static deformation of a membrane structure due to a given volume of ponding water, which will serve as an initial condition for the time varying FSI simulation. One way to simulate this transient interaction between the wind, ponding water and membrane structure is to couple a structural solver modeling the membrane behaviour and a two-phase solver such as a Volume Of Fluid (VOF) solver that simulates the wind and water in a partitioned manner. However, this will be computationally expensive as the fluid domain for simulating the wind is typically huge and requires a large number of cells and the ponding water generally is a small fraction of the wind domain. Therefore, solving multiphase equations in such a large domain with a small volume of ponding water will be computationally inefficient. Therefore, in the current work, we propose a novel coupling strategy to simulate these interactions by considering three solvers for modeling each physical system. Furthermore, considering the small depth and small fetch of the water, relative to the size of the membrane structure, the interaction between the wind and water can be neglected. This results in a coupling strategy where the structural solver interacts with the wind and water solver independently.

The outline of the paper is as following. Section 2 explains the three solver coupling approach and its advantages over the approach where a two-phase is used for modeling the wind and ponding water. The details on the structural and fluid models used given in Section 3. Additionally, gust model used to simulate transient wind is also discussed in this section. Finally, a numerical example is presented in Section 4, where the results from the proposed method is compared with the TPS coupling approach.

2 THREE SOLVER COUPLING

As discussed in Section 1, coupling a two-phase solver, modeling the wind and ponding water, and a structural solver, modeling a membrane structure, is superfluous. Therefore, a new approach is proposed where the three different physical phenomena are simulated using separate numerical models and are coupled in a partitioned manner. This means that during the FSI iterations, the interactions between different pairs of solvers has to be taken into account. Fig. 1 shows the interactions between the three physical systems. First, there is a interaction between the wind and water. The free surface of the water acts as no-slip boundary for the wind (a). The wind on the other hand exerts forces that can cause surface waves (b). Second, there is interaction between the wind and membrane structure (c). Finally, the water and the wetted surface of the membrane surface interact with each other (d). In the current case, due to the small water depth and fetch relative to the size of the membrane, the interaction of the wind and water can be neglected. This makes the coupling tractable. Fig. 2 shows the effect of the assumptions mentioned above on the coupling iterations. In each coupling iteration, the wind and water solver, based on the displacement from the structure, calculate the forces. These forces are first added and supplied to the structural solver to obtain the displacement for the next iteration. To accelerate the convergence, the IQN-ILS algorithm [13] is used. These coupling iterations are performed until convergence is achieved.

This method has several advantages compared to the TPS coupling approach. Firstly, this approach is modular. Therefore, one can use an existing wind simulation set up and include a water solver to observe the influence of ponding. Secondly, a simpler model can be used for

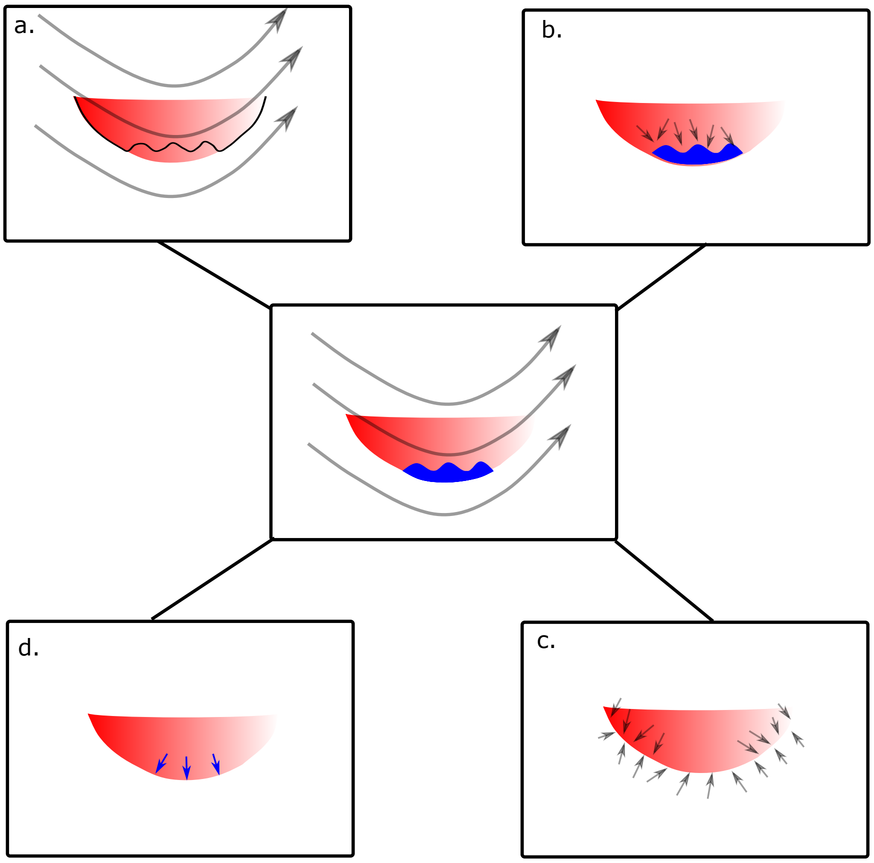

Figure 1: Schematic showing different interactions between the wind, water and membrane structure.

simulating water. For example, for cases where the water is also simulated using the finite volume method, one can use Large Eddy Simulation (LES) for modeling the wind and Unsteady Reynold's Average Navier-Stokes (URANS) for the water, where the time scale is much larger. Lastly, this approach is computationally more efficient. This method avoids solving multiphase equations in the entire wind domain, which is typically large in size. It allows for the use of simpler models computed simultaneously with the wind solver. Therefore, the computational speed will be governed by the most expensive component of the simulation, the wind solver, which is computationally cheaper than the multiphase solver.

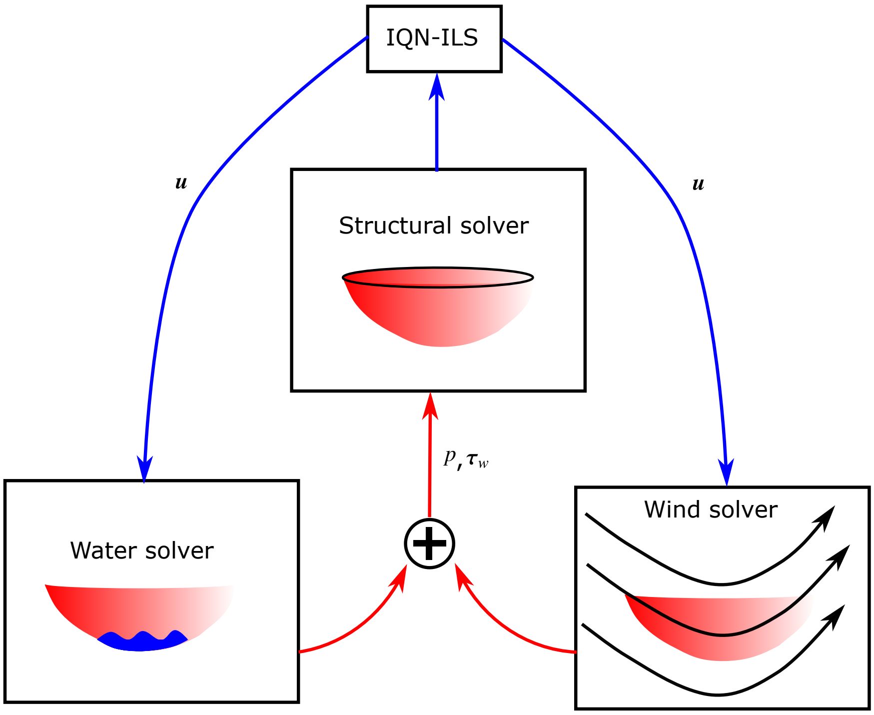

Figure 2: Three solver coupling with exchange of the loads (p, $\boldsymbol{\tau}_w$) and displacement ($\boldsymbol{u}$) at the interface in each coupling iteration.

3 NUMERICAL MODELS

This section discusses the various numerical models used in the proposed coupling approach to simulate the effect of a wind gust on a flexible membrane structure with ponding water, given in Section 4.

3.1 Structural model

The tent structure considered in this work has an edge support and a canopy. The edge supports are considered to be rigid and the canopy is modeled as membrane due to its negligible bending resistance owing to its small thickness. The membrane surface is denoted by Ω_s with thickness t. The variational or weak form of the equilibrium equations for the considered membrane structure can be written as:

$$\int_{\Omega_s} t\,\rho \frac{\partial^2 \boldsymbol{u}}{\partial t^2} \cdot \delta \boldsymbol{u}\, dS + \int_{\Omega_s} t\,\boldsymbol{\sigma} : \delta \boldsymbol{\epsilon}\, dS - \int_{\Omega_s} \boldsymbol{t} \cdot \delta \boldsymbol{u}\, dS = 0, \qquad \forall \delta \boldsymbol{u} \in \mathcal{C}_u \tag{1}$$

where the first term represents the virtual work due to inertia forces, the second term is the internal virtual work and the last term is the external virtual work. The external force $\boldsymbol{t}$ in the considered FSI simulations is the load from the wind and ponding water. The external virtual work from the boundary vanishes due to the rigid edge supports. In Eq. (1), $\boldsymbol{\sigma}$ denotes Cauchy stress, and $\boldsymbol{\delta\epsilon}$ is the virtual Euler strain tensor and $\mathcal{C}_u$ is space of kinematically admissible smooth enough functions. In the current work, we use a displacement based formulation solved using the Finite Element Method, implemented in Kratos [14]. The membrane surface is discretized using bi-linear quadrilateral elements and is integrated in time using second-order Bossak scheme. For the sake of simplicity, the linear elastic plane stress material model is used in the numerical simulations.

3.2 Wind model

3.2.1 Incompressible Navier-Stokes solver

The wind solver used in the proposed coupling approach solves the incompressible single-phase Navier-Stokes (NS) equations. The solution procedure to solve the governing equations is implemented in a finite-volume based open-source code called OpenFOAM. The governing equations for the fluid flow can be written as,

$$\nabla \cdot \boldsymbol{v} = 0 \tag{2}$$

$$\frac{\partial \boldsymbol{v}}{\partial t} + (\boldsymbol{v} - \hat{\boldsymbol{v}}) \cdot \nabla \boldsymbol{v} = -\nabla \tilde{p} + \tilde{\boldsymbol{f}} + 2\nu \nabla \cdot (\nabla_s \boldsymbol{v}), \tag{3}$$

where $\boldsymbol{v}$ and $\tilde{p}$ are the fluid velocity and kinematic pressure. Eq. (2) represents the conservation of mass and Eq. (3) is the momentum equation in Arbitrary Lagrangian Eulerian (ALE) framework with grid velocity $\hat{\boldsymbol{v}}$. The ALE framework is used here because during the FSI iterations, the mesh adapts to the movement of the membrane structure. The operator ∇_s is the symmeteric gradient operator, ν is the kinematic viscosity and $\tilde{\boldsymbol{f}}$ is the force per unit mass.

Eqs (2) and (3) are solved using the Pressure-Implicit with Splitting of Operators (PISO) solution technique with the Crank-Nicolson time integration scheme. For modeling the turbulence, the $k - \epsilon$ turbulence model is used.

3.2.2 Modeling wind gust

In order to simulate an event similar to the Pukkelpop accident, a wind gust needs to be modeled in the wind solver. There are several methods available in the literature to model a wind gust, some examples can be found in [15, 16]. Among the various approaches that are available in the literature, we choose the source term formulation by De Nayer and Breuer [17]. The main advantage of this method is that the gust can created very close to the membrane structure and thus avoiding numerical dissipation before impacting the structure. This source term is added in the momentum equation in a small volume close to the structure, and is written as,

$$\boldsymbol{f}_{gust} = \rho\, \boldsymbol{v}_{total} \cdot \nabla \boldsymbol{v}_{total}, \tag{4}$$

where $\boldsymbol{v}_{total} = \boldsymbol{v} + \boldsymbol{v}_{gust}$ with $\boldsymbol{v}$ as the base wind velocity (without gust) and $\boldsymbol{v}_{gust}$ is the gust velocity. The gust velocity is modeled as product of the gust profile in stream-wise direction ξ, radial direction r, time t and a user-defined amplitude A_g,

$$\boldsymbol{v}_{gust} = A_g f_t(t) f_r(r) f_\xi(\xi) \boldsymbol{e}_\xi. \tag{5}$$

where f_ξ, f_r and f_t are the gust profile in ξ, r and t, respectively. By using Taylor's hypothesis, the time t is directly related to the stream-wise coordinate (ξ). Furthermore, De Nayer and Breuer in their paper state that they only consider the expulsion phase (velocity increase) of the injection because the ingestion phase does not positively contribute to the generation of the gust. If L_g^ξ is the length scale of the gust in stream-wise direction, then the source term after substituting the expression of $\boldsymbol{v}_{gust}$ from Eq. (5) in Eq. (4) with some mathematical manipulations can be written as,

$$\boldsymbol{f}_{gust} = \begin{cases} A_g f_t(t) f_r(r) f_\xi(\xi) \frac{\partial f_\xi}{\partial \xi} & \text{for} \quad \xi \in \left[0, \frac{L_g^\xi}{2}\right] \\ 0 & \text{else} . \end{cases} \tag{6}$$

Depending on the required gust profile, the functions f_ξ, f_r and f_t can be chosen. In the current work, we use the Extreme Coherent Gust (ECG) [18] profile in the radial direction and modified ECG-$\mathcal{C}^2$ [17] in time and stream-wise direction.

3.3 Water model

There are various numerical models or solvers for simulating the behaviour of the ponding water, namely, Material Point Method (MPM), Particle Finite Element Method (PFEM), Smoothened Particle Hydrodynamics (SPH), etc. However, for the sake of ease of implementation in our coupling framework (CoCoNuT), a VOF model with a much smaller domain is used in all the simulations. The governing equations for this VOF model look similar to the incompressible NS equations, Eqs (2) and (3), except here the properties and the fields are written for the fluid mixture. The mixture properties are expressed as a function of the phase fraction of the liquid (in this case, water) α_w, for example, the mixture density ρ_m is written as,

$$\rho_m = \alpha_w \rho_w + (1 - \alpha_w)\,\rho_a, \tag{7}$$

with ρ_w the density of water and ρ_a that of air. To close the equations, a transport equation for phase fraction, Eq (10) is also solved along with NS equations for the fluid mixture. This results in a set of three equations in the ALE framework with grid velocity $\hat{\boldsymbol{v}}$,

$$\frac{\partial \rho_m}{\partial t} + \nabla \cdot (\rho_m \boldsymbol{v}_m) = 0 \tag{8}$$

$$\frac{\partial (\rho_m \boldsymbol{v}_m)}{\partial t} + (\boldsymbol{v}_m - \hat{\boldsymbol{v}}) \cdot \nabla (\rho_m \boldsymbol{v}_m) = -\nabla p + \rho_m \boldsymbol{g} + \boldsymbol{f} + 2\nabla \cdot (\mu_m \nabla_s \boldsymbol{v}_m) + \sigma \kappa \boldsymbol{n}, \tag{9}$$

$$\frac{\partial \alpha_w}{\partial t} + (\boldsymbol{v}_m - \hat{\boldsymbol{v}})\,\nabla \alpha_w + \nabla \cdot [\alpha_w (1 - \alpha_w)\,\boldsymbol{v}_r] = 0, \tag{10}$$

where $\boldsymbol{f}$ is the body force per unit volume. The last term in the right-hand side of Eq (9) is the force due to surface tension which is proportional to the curvature κ and normal vector $\boldsymbol{n}$ of the air-water interface. The proportionality constant σ is called surface tension coefficient, a property of the considered pair of fluids. The additional term in Eq. (10), $\nabla \cdot [\alpha_w (1 - \alpha_w)\,\boldsymbol{v}_r]$ is responsible for obtaining higher resolution of the air-water interface. The equation is solved using a solution technique called Multidimensional Universal Limiter for Explicit Solution (MULES) [19], which bounds the value of α_w between 0 and 1. Like in the case of incompressible NS solver discussed in Section 3.2.1, the PISO solution technique is used to solve Eqs. (8) and (9) with the $k - \epsilon$ turbulence model and the Crank-Nicolson time integration scheme.

4 NUMERICAL EXAMPLE

The numerical example considered in this section is representative of the event that happened during 2011 Pukkelpop festival. However, the data of the tent geometry and its material properties and the volume of ponding water is not available. Therefore, the properties and loading data are chosen so that it represents the actual event qualitatively. We consider a square tent of dimension 6 $m \times 6$ m with all the outer edges fixed. The material property of the membrane is $Et = 10 kN/m$, where E is the Young's Modulus and t is the thickness of the membrane surface. The water volume is chosen such that the wetted area is around 5% of the membrane surface area. By trial and error and using the algorithm for static ponding analysis, developed in our previous work [12], this results in a volume of ponding water $V_f = 0.2\ m^3$. The results from the ponding analysis with $V_f = 0.2\ m^3$ as input is used as a preprocessing step to initialize the fluid and structural domains for transient FSI simulations.

The wind domain around the structure is shown in Fig 3 with all the boundary conditions. The density and kinematic viscosity are taken to be 1 kg/m^3 and $1.48 \times 10^{-5}\ m^2 s^{-2}$, respectively. A uniform inlet velocity $U_{ref} = 10\ m/s$ is applied at the inlet. The gust is injected in a cylindrical region, shown in Fig 3, with the gust amplitude $A_g = 25\ m/s$. As explained in Section 3.2.2, the gust is generated only in the first half of the cylinder region. Initially, the fluid domain is

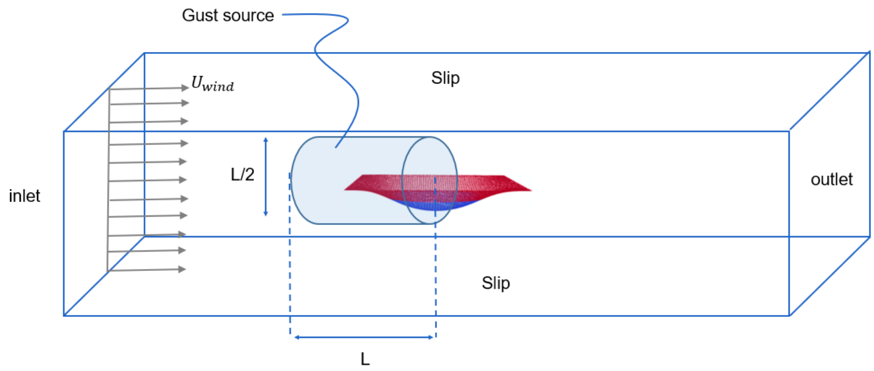

Figure 3: Schematic of the wind domain with boundary conditions around the structure with the region where the gust source is added, where L is the side length of the square membrane.

meshed conforming to the undeformed membrane surface. As a part of the preprocessing step, the displacement field obtained from the static ponding analysis is used to update the membrane surface and the fluid mesh.

The water domain consists of a cube of length L with the flexible membrane as its bottom surface. All the side walls have slip boundary conditions and at the top wall a total pressure $p_0 = 0$ boundary condition is applied. Similar to the wind domain, the cubical domain is meshed with the undeformed membrane surface and subsequently deformed in the preprocessing step. The phase fraction of the water is then initialized based on the free surface height obtained from the static ponding analysis.

The simulation results from the three solver coupling approach is compared with the results obtained using TPS coupling approach. It was observed that the forces from the air in the water domain was in the same range as the forces from the air in the wind domain, especially after the gust traveled through the membrane surface. These forces are the result of added mass from the air, which in the current case was added twice. In order to minimise the forces due to added mass of air in the water domain, a sigmoid scaling function is used to scale the forces in the water domain depending on the phase fraction α_w. When the value of phase fraction on the membrane surface is 1 (completely water), the value of the function is 1 and 0 when $\alpha_w = 0$. The function transitions from 1 to 0 in the range $[\alpha_{w,max}, \alpha_{w,min}]$ and the parameter r controls the smoothness of this transition. It can be written as follows:

$$\sigma(\alpha_{w,max}, \alpha_{w,min}, r) = \frac{1}{1 + e^{-2r(\alpha - \alpha_{mean})/(\alpha_{w,max} - \alpha_{w,min})}}. \tag{11}$$

where $\alpha_{w,mean} = \frac{1}{2}(\alpha_{w,max} + \alpha_{w,min})$. Using the scaling function, one can ensure only the contribution from the water is added. Of course, this filtering is not required when models like MPM, SPH or PFEM are used instead of a VOF model to simulate the ponding water. To compare the results, the vertical displacement of the mid-point is plotted against time, as shown in Fig. 4. For the sake of using short labels in Fig. 4, the three solver coupling is abbreviated as WWS (Wind-water-structure) coupling approach. It can be clearly seen in Fig. 4, the added mass from the air in the water domain plays a significant role and by using a sigmoid scaling of forces led to an improvement in results. The results are further improved when the filtering is

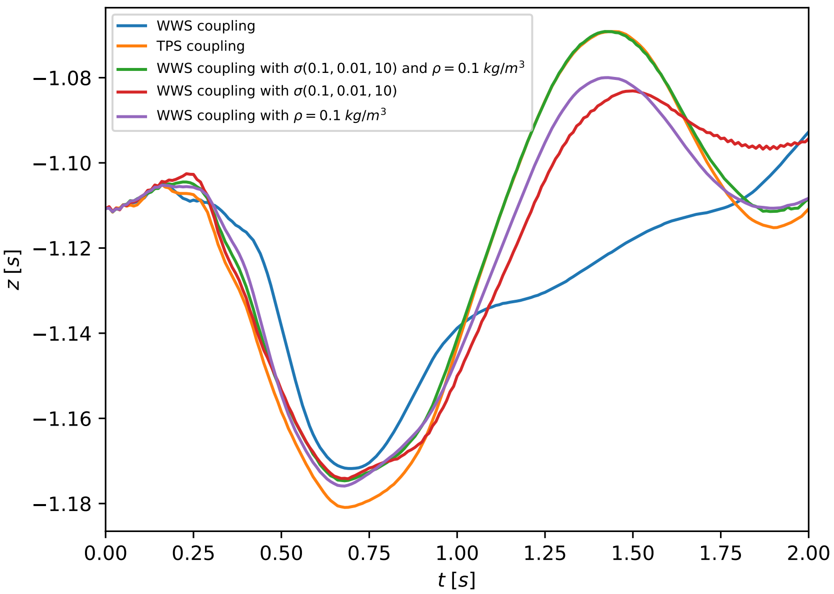

Figure 4: Comparison of the vertical displacement of the midpoint of the tent using various approaches to mitigate the effect of added mass/damping in the water domain. WWS stands for Wind-water-structure coupling or three-solver coupling.

used along with artificially decreasing the density of the air in the water domain. However, it was observed that using the value of density less than 0.1 kg/m^3 led to divergence in the water solver. The VOF model fails when there is a large difference in densities at the interface, which is well-known in the literature.

Finally, some velocity plots at various time steps of the simulation are shown in Fig. 5. Fig. 5a shows the velocity of the wind around the membrane structure when there is no gust. This is followed by Fig. 5b, where the gust wind is developed very close to the membrane structure. The gust then impacts the membrane structure, shown in Fig. 5c and finally, the gust leaves the tent in Fig. 5d.

The computation speed of the three-phase coupling was also compared with the TPS coupling approach. Since the water and wind solvers can be executed in parallel in three solver coupling and the structural solver and coupling operations are only a fraction of the overall cost, the average computing time of the wind solver (most expensive) in every time step is used for comparison. This is compared with the average computing time of the two-phase solver in every time step. It was found that the computing time of the TPS coupling approach was around 20% higher than the three solver coupling approach.

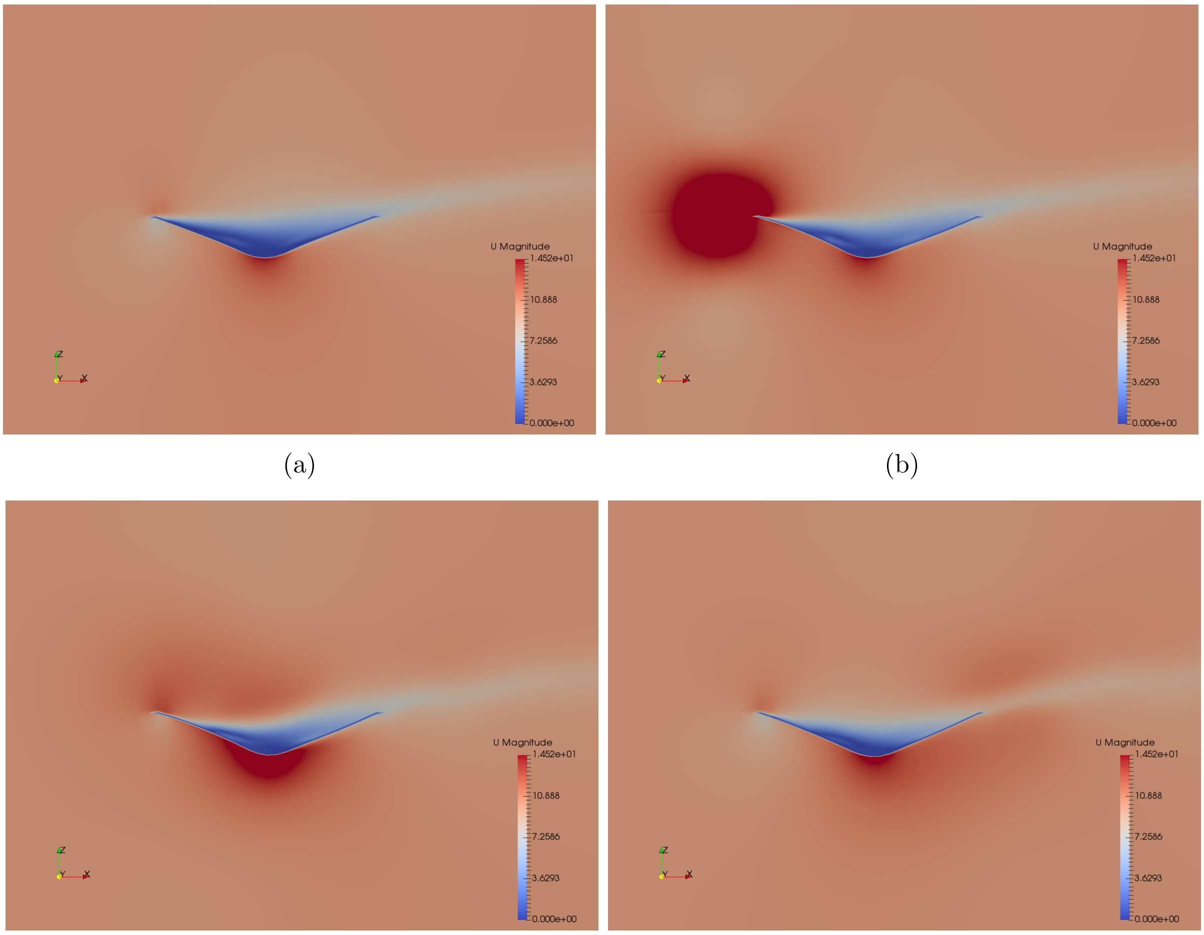

(a) (b) (c) (d)

Figure 5: Snapshots of gust striking the flexible tent a) Uniform flow without the gust, b) generation of the gust in localized region c) gust striking the tent, d) gust leaving the tent structure.

5 CONCLUSIONS

A novel coupling approach was proposed to simulate the wind induced movement of the membrane structure with some ponding water. It uses separate solvers or models for modeling the flexible membrane structure, wind and water. With the assumptions that the wind-water interaction is negligible due to small fetch and water depth, the coupling process was simplified. It was found that the results from the three solver coupling agreed well with the TPS coupling approach when the added mass of air in the water domain was minimized. This added mass was present because the VOF model was used to simulate water with still air. Using other models like MPM, SPH or PFEM should work without any modifications. It was also found that the performance of the three solver coupling approach in terms of computing time is better than the TPS coupling approach.

REFERENCES

[1] P. D. Meutter, L. Gerard, G. Smet, K. Hamid, R. Hamdi, D. Degrauwe, P. Termonia, Predicting small-scale, short-lived downbursts: Case study with the NWP limited-area ALARO model for the pukkelpop thunderstorm, Monthly Weather Review 143 (3) (2015) 742–756. doi:10.1175/mwr-d-14-00290.1.

[2] R. Wüchner, A. Kupzok, K.-U. Bletzinger, A framework for stabilized partitioned analysis of thin membrane–wind interaction, International Journal for Numerical Methods in Fluids 54 (6-8) (2007) 945–963. doi:10.1002/fld.1474.

[3] A. Michalski, B. Gawenat, P. Gelenne, E. Haug, Computational wind engineering of large umbrella structures, Journal of Wind Engineering and Industrial Aerodynamics 144 (2015) 96–107. doi:10.1016/j.jweia.2015.05.002.

[4] N. Aubin, B. Augier, P. Bot, F. Hauville, R. Floch, Inviscid approach for upwind sails aerodynamics. How far can we go?, Journal of Wind Engineering and Industrial Aerodynamics 155 (2016) 208–215. doi:10.1016/j.jweia.2016.06.005.

[5] G. D. Nayer, A. Apostolatos, J. Wood, K. Bletzinger, R. Wüchner, M. Breuer, Numerical studies on the instantaneous fluid-structure interaction of an air-inflated flexible membrane in turbulent flow, Journal of Fluids and Structures 82 (2018) 577–609. doi:10.1016/j.jfluidstructs.2018.08.005.

[6] C. Antoci, M. Gallati, S. Sibilla, Numerical simulation of fluid-structure interaction by SPH, Computers & Structures 85 (11-14) (2007) 879–890. doi:10.1016/j.compstruc.2007.01.002.

[7] W. A. Wall, S. Genkinger, E. Ramm, A strong coupling partitioned approach for fluid–structure interaction with free surfaces, Computers & Fluids 36 (1) (2007) 169–183. doi:10.1016/j.compfluid.2005.08.007.

[8] S. R. Idelsohn, J. Marti, A. Souto-Iglesias, E. Oñate, Interaction between an elastic structure and free-surface flows: experimental versus numerical comparisons using the PFEM, Computational Mechanics 43 (1) (2008) 125–132. doi:10.1007/s00466-008-0245-7.

[9] J. Degroote, A. Souto-Iglesias, W. V. Paepegem, S. Annerel, P. Bruggeman, J. Vierendeels, Partitioned simulation of the interaction between an elastic structure and free surface flow, Computer Methods in Applied Mechanics and Engineering 199 (33-36) (2010) 2085–2098. doi:10.1016/j.cma.2010.02.019.

[10] K. Liao, C. Hu, M. Sueyoshi, Free surface flow impacting on an elastic structure: Experiment versus numerical simulation, Applied Ocean Research 50 (2015) 192–208. doi:10.1016/j.apor.2015.02.002.

[11] Z. Sun, Z. Huang, X. Zhou, Benchmarking the material point method for interaction problems between the free surface flow and elastic structure, Progress in Computational Fluid Dynamics, an International Journal 19 (1) (2019) 1–11.

[12] N. Narayanan, R. Wüchner, J. Degroote, Monolithic and partitioned approaches to determine static deformation of membrane structures due to ponding, Computers & Structures 244 (2021) 106419. doi:10.1016/j.compstruc.2020.106419.

[13] J. Degroote, R. Haelterman, S. Annerel, P. Bruggeman, J. Vierendeels, Performance of partitioned procedures in fluid–structure interaction, Computers & Structures 88 (7-8) (2010) 446–457. doi:10.1016/j.compstruc.2009.12.006.

[14] P. Dadvand, R. Rossi, E. Oñate, An object-oriented environment for developing finite element codes for multi-disciplinary applications, Archives of computational methods in engineering 17 (3) (2010) 253–297. doi:10.1007/s11831-010-9045-2.

[15] W. Bierbooms, Specific gust shapes leading to extreme response of pitch-regulated wind turbines, Journal of Physics: Conference Series 75 (2007) 012058. doi:10.1088/1742-6596/75/1/012058.

[16] R. Bos, Extreme gusts and their role in wind turbine design, Ph.D. thesis (2017). doi:10.4233/uuid:d6097e3a-1cdd-4845-a71c-90f469d28b7a.

[17] G. D. Nayer, M. Breuer, A source-term formulation for injecting wind gusts in CFD simulations, Journal of Wind Engineering and Industrial Aerodynamics 207 (2020) 104405. doi:10.1016/j.jweia.2020.104405.

[18] I. Standard, 61 400-21: Measurement and assessment of power quality of grid connected wind turbines, International Electrotechnical Commission. F1147-E (12/2004).

[19] S. M. Damián, An extended mixture model for the simultaneous treatment of short and long scale interfaces, Ph.D. thesis (2013). doi:10.13140/RG.2.1.3182.8320.